NJC

Cite this: *New J. Chem.*, 2012, **36**, 575–587

www.rsc.org/njc

PAPER

Antioxidant activity of (all-*E*)-lycopene and synthetic apo-lycopenoids in a chemical model of oxidative stress in the gastro-intestinal tract†

Pascale Goupy,[ab] Eric Reynaud,[ab] Olivier Dangles[ab] and Catherine Caris-Veyrat*[ab]

Received (in Montpellier, France) 23rd May 2011, Accepted 30th October 2011
DOI: 10.1039/c1nj20437h

Lycopene, the main pigment of tomato, is known to have protective effects on health. Its metabolites could also be involved in these effects. Potentially bioactive lycopene metabolites namely apo-10′-lycopenol, apo-10′-lycopenal, apo-14′-lycopenol, apo-14′-lycopenal, and apo-11-lycopenoids with alcohol, carboxylic acid, aldehyde and ethyl ester terminal groups were obtained by organic synthesis as (all-*E*) stereoisomers using HWE condensation reactions. The ability of (all-*E*)-lycopene and the synthesized apo-lycopenoids to inhibit lipid peroxidation was tested in a chemical model of postprandial oxidative stress in the gastric compartment. Oxidative stress was generated by metmyoglobin, the main form of dietary iron (from red meat), which is able to catalyse the peroxidation of linoleic acid under mildly acidic conditions. In this model, apo-6′-lycopenal and apo-8′-lycopenal were better inhibitors of lipid peroxidation than (all-*E*)-lycopene itself. For the apo-lycopenoids, a long unsaturated chain and a terminal carboxylic acid group both favour the antioxidant activity. The short-chain apo-lycopenoic acid, apo-14′-lycopenoic acid, was shown to behave like a hydrophilic antioxidant, *i.e.* by reducing hypervalent iron forms of metmyoglobin. Thus, besides the polyene chain length, the terminal group of the apo-lycopenoids is expected to deeply influence the lipophilic/hydrophilic balance of the molecule (and consequently its distribution between the aqueous and lipid phases) and its affinity for the heme cavity. It can thus be concluded that the polyene chain length and terminal group are two important parameters modulating the mechanism by which apo-lycopenoids express their antioxidant activity.

Introduction

Dietary intake of tomatoes and tomato-derived products has been shown to be associated with a lower risk of chronic diseases such as cancer or cardiovascular disease.[1–4] Lycopene (Table 1), the main carotenoid pigment of tomato, could be involved in these protective effects, however mechanisms underlying its biological activity *in vivo* are not fully elucidated. Lycopene metabolites are supposed to participate in the biological effects attributed to lycopene.[6]

The antioxidant activity of carotenoids is one possible mechanism underlying the beneficial effects of carotenoids *in vivo*.[7,8] β-Carotene is indeed an essential antioxidant in green plants, protecting them from singlet dioxygen produced in excess of light. *In vitro*, lycopene has been shown to be the most efficient carotenoid for the quenching of singlet dioxygen.[9] However, the antioxidant activity of carotenoids in humans has not yet been clearly shown and is still a matter of debate.[10] A major problem is the low concentration of carotenoids in plasma, at most of the order of 1 μM, or in organs (compared with recognized antioxidants like α-tocopherol in prostate)[11] as a result of their limited absorption through the intestinal barrier. However, in humans, it has been demonstrated that lycopene concentrations in the stomach could reach 50 μM only 20 min after ingestion of a meal containing 33.6 g of tomato purée (10 mg of lycopene).[12] The gastric concentration of lycopene was still 40 μM and 25 μM after 1 h and 2 h, respectively. Thus, it has been hypothesized that the antioxidant action of poorly bioavailable micronutrients like carotenoids and polyphenols could be relevant mainly in the gastro-intestinal tract.[13,14] Indeed, lipid peroxidation induced by dietary iron can be quite fast in the gastric compartment due to the presence of nonlimiting dioxygen concentrations and to the acidic pH, which makes iron ions more redox-active. Besides the loss of essential fatty acids, the peroxidation of dietary polyunsaturated lipids has the additional drawback of producing bioavailable and potentially toxic lipid oxidation products, which are considered possible risk factors in atherogenesis.[15]

Hence, an experimental model of oxidative stress in the gastro-intestinal tract may be a biologically relevant model for mimicking the antioxidant activity of carotenoids *in vivo*.[13,16]

[a] *INRA, UMR408 Safety and Quality of Plant Products, F-84000 Avignon, France. E-mail: catherine.caris@avignon.inra.fr; Fax: +33 (0)4-32-72-24-92; Tel: +33 (0)4-32-72-24-89*
[b] *University of Avignon, UMR408, F-84000 Avignon, France*
† Electronic supplementary information (ESI) available. See DOI: 10.1039/c1nj20437h

Table 1 Chemical structures of (all-*E*)-lycopene and the apo-lycopenoids investigated

Compounds	Short name	Molecular Structure	λ_{max} nm in $CHCl_3$[a]
(All-*E*)-lycopene (31)[c]	**(all-*E*)-lyc.**	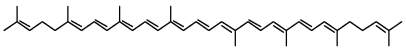	458, 485, 518, %III/II = 60
Apo-11-lycopenal	**11-CHO**	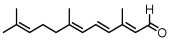	345
Apo-11-lycopenoic acid	**11-COOH**	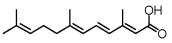	276, sh[b] 323
Apo-11-lycopenol	**11-CH_2OH**	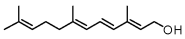	sh 276, 286, sh 297
Ethyl apo-11-lycopenoate	**11-COOEt**	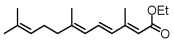	318
Apo-14′-lycopenal	**14′-CHO**	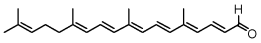	422
Apo-14′-lycopenoic acid	**14′-COOH**	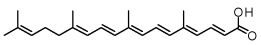	410
Apo-14′-lycopenol	**14′-CH_2OH**	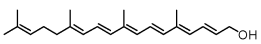	375, 387, 398, %III/II = 64
Methyl apo-14′-lycopenoate	**14′-COOMe**	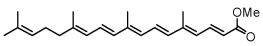	411
Apo-12′-lycopenal	**12′-CHO**	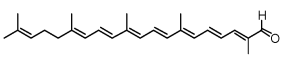	454
Apo-10′-lycopenal	**10′-CHO**	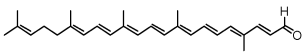	474
Apo-10′-lycopenoic acid (504.4)[c]	**10′-COOH**	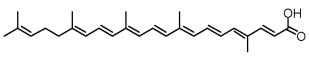	454
Apo-10′-lycopenol (504.3)[c]	**10′-CH_2OH**	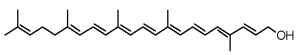	405, 427, 457, %III/II = 79
Ethyl apo-10′-lycopenoate	**10′-COOEt**	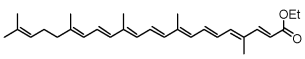	455
Apo-8′-lycopenal (491)[c]	**8′-CHO**	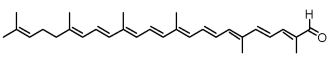	486
Apo-6′-lycopenal (471)[c]	**6′-CHO**	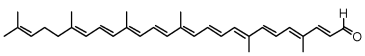	504

[a] Main maximum underlined. [b] Shoulder. [c] Name and/or number from Carotenoids Handbook.[5]

Lycopene-derived products are believed to play a key role in biological effects once attributed only to lycopene.[6,17] Lycopene metabolites formed by oxidative cleavage of the hydrocarbon chain (apo-lycopenoids) have been found in animals fed lycopene-enriched diets, like apo-8′-lycopenal and apo-12′-lycopenal in rat liver[18] and apo-10′-lycopenol in lung of ferrets possibly issued from a cleavage of (5-*Z*) and (13-*Z*) lycopene isomers by intestinal carotenoid monoxygenase (CMO2).[19] Apo-10′-lycopenal could be converted to both alcohol (apo-10′-lycopenol) and acid (apo-10′-lycopenoic acid) in the presence of NADPH and a post-nuclear fraction of ferret liver. More recently, apo-6′-, apo-8′-, apo-10′-, apo-12′-, apo-14′- and apo-15′-lycopenals were detected in the plasma of humans who had consumed tomato juice.[20] Interestingly, these apo-lycopenals have also been found in food products, especially in processed food (*e.g.*, tomato paste) where they are more concentrated than in fresh food as a consequence of plant tissue disruption during processing.[20] Hence, so far, one cannot conclude that apo-lycopenoids are authentic human metabolites of lycopene.

Several lycopene-derived molecules have been shown to be biologically active *in vitro*. Acyclo-retinoic acid (apo-15′-lycopenoic acid), the linear analogue of retinoic acid, which is formally issued from a central cleavage of lycopene, was shown to increase gap junction communication, although only at high concentrations.[21] Apo-10′-lycopenoic acid, a metabolite issued from an excentric oxidative cleavage of lycopene, has been shown to inhibit lung carcinogenesis both *in vivo* and *in vitro*, *via* the activation of the Nrf2 transcription factor and the induction of phase II detoxifying/antioxidant enzymes.[22] Dialdehydes formed by double oxidative cleavage of the carotenoid chain have been shown to be more potent than lycopene at activating the antioxidant response element (ARE) transcription system.[23] It was thus shown that lycopene metabolites might induce phase-II enzymes by the same mechanism as the one demonstrated for carotenoids[24] and even more efficiently.

Recently, we demonstrated that apo-14′-lycopenoic acid and apo-10′-lycopenoic acid are potential endogenous lycopene metabolites involved in the activation of hormone receptors and in the regulation of CMO1 and CMO2 expression.[25]

While the antioxidant effect of lycopene has been extensively studied, similar data on lycopene metabolites are scarce. In one study a decrease in endogenous reactive oxygen species (ROS) production has been observed after treatment of BEAS-2B cells with apo-10′-lycopenoic acid, suggesting a possible indirect antioxidant effect.[22,26] To our knowledge, direct antioxidant effects of lycopene metabolites have not been described yet.

The aim of the present study was to study the ability of (all-*E*)-lycopene and apo-lycopenoids with different chain lengths and terminal groups (alcohol, aldehyde, carboxylic acid and ester) to inhibit lipid peroxidation in a simple chemical model of postprandial oxidative stress in the gastric compartment.[16] Oxidative stress was generated by metmyoglobin, one of the main forms of dietary iron (red meat), which is able to catalyse the peroxidation of linoleic acid in mildly acidic conditions. This model allowed us to demonstrate that hydrophilic and lipophilic antioxidants display distinct inhibition mechanisms[27] and more recently was used to discriminate the antioxidant action of red wine pigments with close structures.[28]

Results and discussion

Synthesis of apo-11-, apo-14′- and apo-10′-lycopenoids

We have previously obtained apo-lycopenoids by direct oxidation of lycopene with $KMnO_4$.[29] More recently, we described the organic synthesis of apo-10′-lycopenoic acid (**10′-COOH**) and apo-14′-lycopenoic acid (**14′-COOH**) and their corresponding methyl or ethyl esters.[25] In the present work, a similar strategy based on the Horner–Wadsworth–Emmons (HWE) reaction was developed to build the hydrocarbon skeleton of apo-11-lycopenoids (Table 1). Reduction and subsequent oxidation reactions were applied to the apo-lycopenoic esters of the 14′ and 10′ series previously obtained in order to prepare the corresponding apo-lycopenols, apo-lycopenals and apo-lycopenoic acids (Table 1). Special attention was paid to obtaining apo-lycopenoids of (all-*E*) configuration.

Apo-11-lycopenoids. Ethyl apo-11-lycopenoate (**11-COOEt**) was prepared by elongation of the carbon chain of pseudo-ionone (**PI**) upon treatment with one equivalent of triethyl-phosphonoacetate (HWE reaction) (Scheme 1). The mechanism of this condensation involves a cyclic phosphate intermediate and leads to a new carbon–carbon double bond with a diastereo-isomeric (*E*/*Z*) ratio of 3.5 and a yield of 82%. Silica gel chromatography did not allow us to efficiently separate the **11-COOEt** diastereoisomers, so the crude mixture was reduced using DIBAH. After purification by silica gel chromatography, apo-11-lycopenol (**11-CH_2OH**) was obtained as an (*E*) isomer (purity 97%, 3% (*Z*) isomer) with a yield of 16%. A diastereo-isomeric mixture of **11-CH_2OH** was used for the preparation of apo-11-lycopenal (**11-CHO**) by oxidation of the allylic alcohol. After purification by silica gel chromatography, **11-CHO** was obtained in 30% yield as an (*E*) isomer (purity 96%, 4% (*Z*) isomer). Finally, apo-11-lycopenoic acid (**11-COOH**) was obtained as a pure (*E*) isomer by mild oxidation of **11-CHO** using Ag_2O with a yield of 90%. Saponification of crude **11-COOEt** gave a diastereoisomeric mixture of **11-COOH** that could not be purified to obtain the pure (*E*) isomer.

Apo-14′-lycopenoids. Reduction of methyl apo-14′-lycopenoate[25] (**14′-COOMe**) by DIBAH and subsequent crystallization provided pure (*E*) apo-14′-lycopenol (**14′-CH_2OH**) in 35% yield (Scheme 2A). Apo-14′-lycopenal (**14′-CHO**) was obtained as a pure (*E*) isomer by oxidation of **14′-CH_2OH** using MnO_2 with a yield of 44%.

Apo-10′-lycopenoids. Apo-10′-lycopenol (**10′-CH_2OH**) was obtained by reduction of ethyl apo-10′-lycopenoate[25] (**10′-COOEt**) in the presence of an excess of the mild reducing agent DIBAH (Scheme 2B). After purification, **10′-CH_2OH** was obtained with a yield of 31% as a pure (*E*) isomer. Oxidation of **10′-CH_2OH** using an excess of MnO_2 in ethyl acetate provided apo-10′-lycopenal (**10′-CHO**), which was crystallized in a pure (*E*) isomer with a yield of 44%.

Spectral characteristics of (all-*E*)-lycopene and apo-lycopenoids

(All-*E*)-lycopene displays a UV-visible spectrum with a typical three-band (I–III) fine structure (458, 485, 518 nm, in $CHCl_3$, %III/II = 60) (Fig. 1 and Table 1). This fine structure is also present in the UV-visible spectrum of **10′-CH_2OH** (%III/II = 79) and the shorter apo-lycopenol **14′-CH_2OH** (%III/II = 64), whereas it has almost completely disappeared in the shortest apo-lycopenol **11-CH_2OH** (Fig. 1A). Thus, the vibrational fine structure of lycopene is maintained in the longest apo-lycopenols only. By contrast, the fine structure is strongly weakened in the UV-visible spectra of apo-lycopenoic acids and esters and has completely disappeared in the spectra of apo-lycopenals as shown

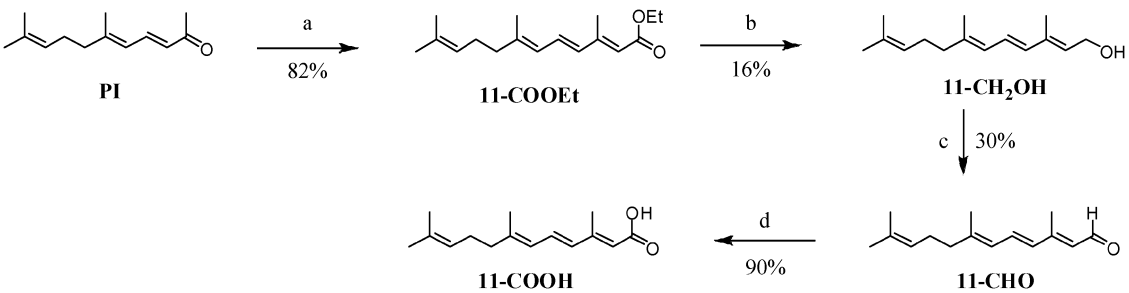

Scheme 1 Synthesis of ethyl apo-11-lycopenoate (**11-COOEt**), apo-11-lycopenol (**11-CH_2OH**), apo-11-lycopenal (**11-CHO**) and apo-11-lycopenoic acid (**11-COOH**). *Reagents and conditions*: (a) triethylphosphonoacetate, NaH, THF; (b) DIBAH, THF; (c) MnO_2, AcOEt; and (d) Ag_2O, NaOH, EtOH.

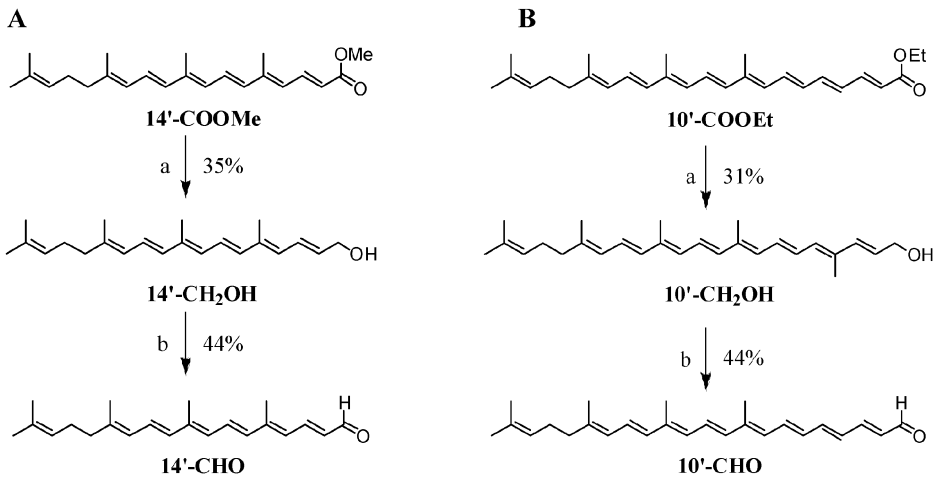

Scheme 2 (A) Synthesis of apo-14′-lycopenol (**14′-CH_2OH**) and apo-14′-lycopenal (**14′-CHO**). (B) Synthesis of apo-10′-lycopenol (**10′-CH_2OH**) and apo-10′-lycopenal (**10′-CHO**). *Reagents and conditions*: (a) DIBAH, THF; (b) MnO_2, AcOEt.

for apo-10′-lycopenoids (Fig. 1B, results not shown for the other apo-lycopenoid series). It is known that conjugation of the polyene chromophore of carotenoids to a carbonyl group induces a loss of the vibrational fine structure (though in nonpolar solvents the fine structure may be retained).[30] The maximum absorption wavelength increases in the series **10′-CH_2OH** (405, 427, 457 nm), **10′-COOH** (454 nm), **10′-COOEt** (455 nm) and **10′-CHO** (474 nm). These results reflect the conjugation of the carbonyl group with the polyene chain and the stronger attractive mesomeric effect of an aldehyde *vs.* a carboxylic acid or ester. Moreover, the difference in λ_{max} values between **10′-CHO** and **10′-CH_2OH** is higher than that observed between apo-10′-β-carotenal (434 nm) and apo-10′-β-carotenol (386, 408, 432 nm)[30] in ethanol (47 nm *vs.* 26 nm). This difference might be explained by restrictions in conjugation brought about by the cyclic terminal group of apo-β-carotenoids and by the different solvents used (chloroform *vs.* ethanol).

As expected, a clear hypsochromic shift is observed for apo-lycopenals (Fig. 1C) when the number of conjugated double bonds decreases with λ_{max} values going from 504 nm for apo-6′-lycopenal to 345 nm for apo-11-lycopenal. Simultaneously, a hypochromic shift is also observed.

Inhibition of linoleic acid peroxidation

(All-*E*)-lycopene and apo-lycopenoids were assayed for their ability to inhibit the peroxidation of linoleic acid induced by dietary heme iron (metmyoglobin) in a mildly acidic micellar solution. The selected pH of 5.8 is representative of the gastric compartment during the early step of digestion[12] when oxidative processes are most likely to take place. The accumulation of conjugated dienes (CDs, mainly lipid hydroperoxides[16]) as primary products of lipid oxidation was monitored by UV-visible spectroscopy at 234 nm in the absence (uninhibited peroxidation) or presence of (all-*E*)-lycopene or apo-lycopenoids at different concentrations. Simultaneously, the consumption of the antioxidants displaying a convenient UV-visible absorption ($\lambda \geq 400$ nm) was also monitored (see for example results for **8′-CHO** in Fig. 2). The A(234 nm) *vs.* time curve of uninhibited peroxidation is quasi-linear with a peroxidation rate (R_p^0) of *ca.* 130 nM s^{-1} (Fig. 2). In the presence of lycopene and the apo-lycopenoids, the accumulation of CDs proceeds according to two phases: a lag phase followed by a propagation phase (Fig. 2). The antioxidant markedly slows down the accumulation of CDs during the lag phase whose duration increases with the antioxidant concentration and reflects the period during which most of the carotenoid is consumed (Fig. 2). Similar kinetic profiles were observed for all apo-lycopenoids as shown in Fig. 3 for the apo-10′- and apo-14′-series, except for apo-11-lycopenoids, which are poor antioxidants in this model (results not shown). However, significant differences between short-chain and long-chain apo-lycopenoic acids can be outlined. Indeed, whereas **10′-COOH** exerts its inhibitory activity mainly by prolonging the lag phase, **14′-COOH** partly inhibits the peroxidation by lowering the rate of the propagation phase (Fig. 3A), which might indicate a different inhibition mechanism (see below). It is also remarkable that, at the end of the lag phase, short-chain antioxidants (14′ series) are more spared than long-chain analogues, which typically are totally consumed (Table 2).

Control experiments without linoleic acid (LH) or metmyoglobin ($MbFe^{III}$) or both were carried out. For each antioxidant (initial concentration = 10 μM, except lycopene, 2 μM), the percentage of consumption was evaluated at a fixed time period corresponding to the end of the lag phase of metmyoglobin-induced lipid peroxidation. A non-negligible consumption of (all-*E*)-lycopene and apo-lycopenoids (between 7 to 17%) was observed in the phosphate buffer containing 2 mM Tween 20 at pH 5.8 and 37 °C under gentle stirring (Table 2). In such conditions, antioxidant degradation could be due to photo-oxidation and/or autoxidation initiated by metal ion traces present in buffer and peroxides contaminating Tween 20.[31] Linoleic acid or $MbFe^{III}$ alone slightly accelerates apo-lycopenoid consumption. This could reflect the slow reduction of $MbFe^{III}$ into $MbFe^{II}$ (myoglobin) by the antioxidants and the 'spontaneous' co-oxidation of linoleic acid and antioxidants. By contrast, the simultaneous presence of LH and $MbFe^{III}$ dramatically accelerates apo-lycopenoid consumption, thus indicating that this process essentially reflects the inhibition by apo-lycopenoid of the metmyoglobin-induced peroxidation of linoleic acid. For apo-lycopenals, the longer the chain length, the longer the lag

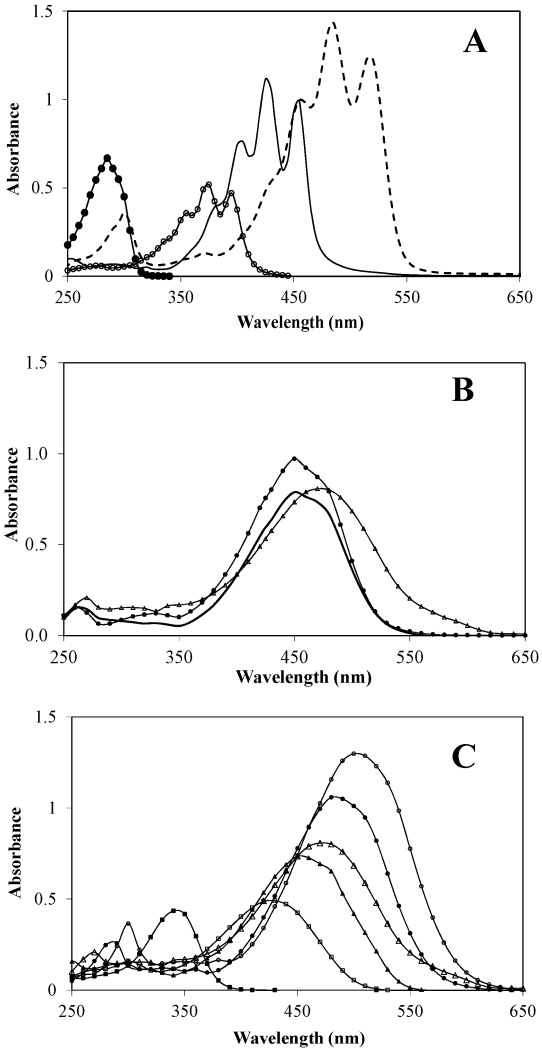

Fig. 1 UV-visible spectra of (all-*E*)-lycopene and apo-lycopenoids in $CHCl_3$. Concentration was 10 μM except for **11-CH_2OH**, 25 μM. (A) (All-*E*)-lycopene (dotted line) and apo-lycopenols: **10′-CH_2OH** (full line); **14′-CH_2OH** (circles); **11-CH_2OH** (full circles). (B) Apo-10′-lycopenoids series: **10′-COOEt** (full circles); **10′-CHO** (triangles); **10′-COOH** (full line). (C) Apo-lycopenals: **6′-CHO** (circles); **8′-CHO** (full circles); **10′-CHO** (triangles); **12′-CHO** (full triangles); **14′-CHO** (squares); **11-CHO** (full squares).

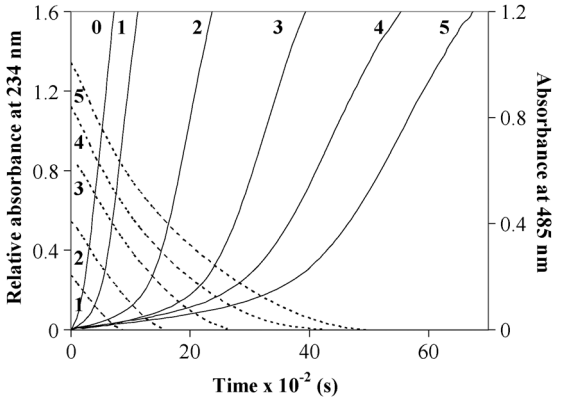

Fig. 2 Accumulation of conjugated dienes (full lines, detection at 234 nm) and simultaneous consumption of the antioxidant (dotted lines, detection at 485 nm) during the metmyoglobin-induced peroxidation of linoleic acid in the presence of **8′-CHO**. **8′-CHO** concentrations are: 0 (**0**), 2 (**1**), 4 (**2**), 6 (**3**), 8 (**4**) and 10 μM (**5**). Linoleic acid (0.7 mM), metmyoglobin (100 nM), pH 5.8 phosphate buffer containing 2 mM Tween 20, 37 °C.

phase, the longer the half-life of the antioxidant and the higher the extent of antioxidant consumption at the end of the lag phase. Within both 10′ and 14′ series, the lag phase of peroxidation and half-life of the antioxidant both increase as follows: apo-lycopenol < apo-lycopenoate < apo-lycopenal < apo-lycopenoic acid. Those trends reflect the relative efficiency of the selected antioxidants.

For a global estimation of the antioxidant efficiency based on both the lag and propagation phases and involving several antioxidant concentrations, a IC_{50} parameter was calculated as follows. For each antioxidant concentration C, T is defined as the period of time needed to accumulate a given CD concentration after addition of $MbFe^{III}$ (*e.g.*, that corresponding to a 0.7 increase in the absorbance at 234 nm from its value at time zero). In the absence of antioxidant, T becomes T_0. For a fixed antioxidant concentration, a larger $\Delta T = T - T_0$ means a higher antioxidant activity (Fig. 4). For each concentration tested, differences between antioxidants were significant, except for **14′-CHO** and **12′-CHO**. Moreover, due a slight curvature in the T *vs.* antioxidant concentration (C), T can be satisfactorily fitted against a quadratic function of C (not shown): $T/T_0 = 1 + aC + bC^2$ to extract a IC_{50} value for each antioxidant. IC_{50} parameter is defined as the antioxidant concentration leading to $T = 2T_0$: $IC_{50} = (\sqrt{(a^2 + 4b)} - a)/2b$.[28] The lower the IC_{50} value, the more effective the antioxidant. It is noteworthy that two apo-lycopenoids are more antioxidant than lycopene itself: **6′-CHO** followed by **8′-CHO** (Table 3). High IC_{50} values of apo-11-lycopenoids confirm their very low antioxidant activity. More importantly, comparisons based on ΔT (Fig. 4) or on IC_{50} both lead to the same conclusions: apo-lycopenals with longer chains are more antioxidant than shorter ones. Although limited to a smaller number of antioxidants, the same trend is observed for acids, alcohols and esters. For a fixed chain length (10′ and 14′ series), the influence of the terminal group on the antioxidant activity is: alcohol < ester ≤ aldehyde < carboxylic acid. It must be outlined that apo-lycopenoic acids are amphiphilic antioxidants with an anionic carboxylate end. Their likely location at the interface of micelles seems to improve their efficiency at inhibiting the peroxidation mechanism.

Mechanisms of inhibition

Theoretical considerations. HOMO energies (E(HOMO)) of lycopene and apo-lycopenoids were estimated by semi-empirical quantum mechanics calculations as an approximation of the ionisation potential (I_p): $I_p = -E$(HOMO). The I_p value is a measure of the intrinsic electron-donating capacity. For apo-lycopenals, the longer the chain length, the lower the ionisation potential and the lower the IC_{50} (Table 3). This correlation suggests that the antioxidant activity of apo-lycopenals may be directly linked to their reducing capacity. This is also true for esters. However, for the same chain length (10′, 14′ and 11 series), acids, esters and aldehydes have very similar ionisation potentials, whereas I_p values are lower for apo-lycopenols. This trend is

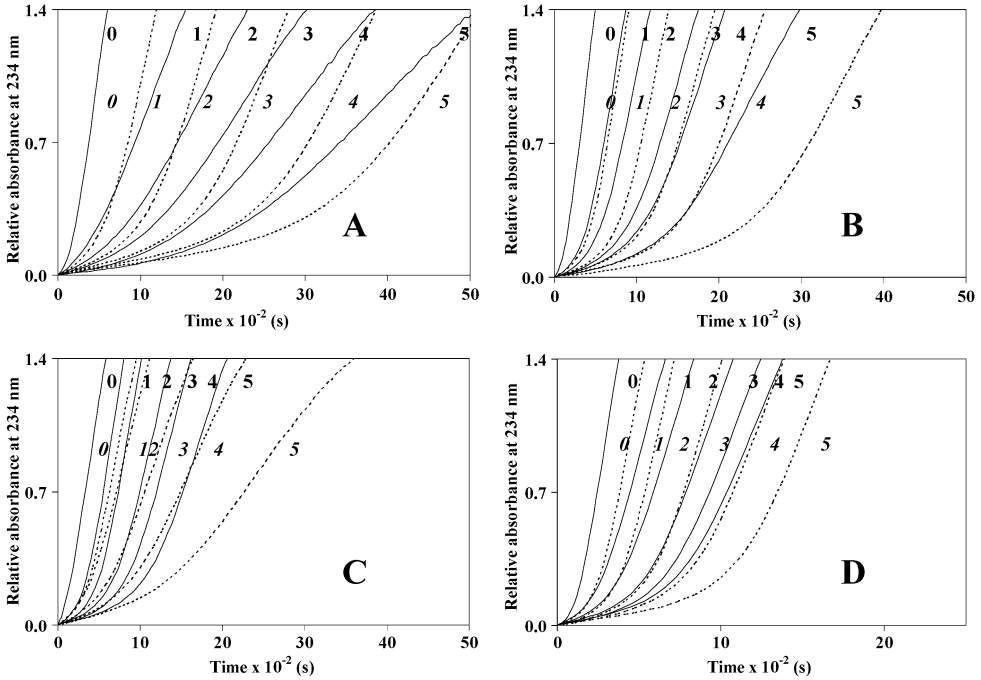

Fig. 3 Accumulation of conjugated dienes (detection at 234 nm) during inhibition of the metmyoglobin-induced peroxidation of linoleic acid by apo-14′-lycopenoids (full lines, numbers in normal) and apo-10′-lycopenoids (dotted lines, numbers in italic). Apo-lycopenoids concentrations are: 0 (**0**), 2 (**1**), 4 (**2**), 6 (**3**), 8 (4) and 10 μM (**5**). Linoleic acid (0.7 mM), metmyoglobin (100 nM), pH 5.8 phosphate buffer containing 2 mM Tween 20, 37 °C. (A) Inhibition by apo-lycopenoic acids. (B) Inhibition by apo-lycopenals. (C) Inhibition by apo-lycopenoates. (D) Inhibition by apo-lycopenols.

Table 2 Kinetic parameters of antioxidant (AO) consumption at pH 5.8 and 37 °C (detection at the maximum absorption wavelength of each compound). Initial concentrations: antioxidant (C_{AOi}), 10 μM, except **(all-*E*)-lyc.**, 2 μM, Tween 20, 2 mM, LH, 0.7 mM, $MbFe^{III}$, 100 nM

		% AO[b] consumed at the end of the lag phase[c]					
Compound	λ_{max}/nm[a]	Without LH and $MbFe^{III}$	With LH alone	With $MbFe^{III}$ alone	With LH and $MbFe^{III}$	Half-life of antioxidant[b,d]/s	Lag phase[b,c]/s
(all-*E*)-lyc.	480	8 ± 0	18 ± 4	34 ± 1	94 ± 0	158 ± 27	375 ± 28
6′-CHO	504	17 ± 1	42 ± 2	30 ± 1	98 ± 1	1389 ± 37	3626 ± 112
8′-CHO	485	16 ± 1	39 ± 7	27 ± 1	92 ± 1	1274 ± 37	2398 ± 204
10′-CHO	454	14 ± 1	20 ± 1	22 ± 3	96 ± 2	1001 ± 129	1612 ± 110
12′-CHO	454	13 ± 4	21 ± 2	23 ± 2	76 ± 2	832 ± 37	1429 ± 202
14′-CHO	426	10 ± 1	14 ± 1	15 ± 1	60 ± 1	849 ± 19	1066 ± 44
10′-COOH	440	16 ± 1	25 ± 3	35 ± 2	88 ± 1	1089 ± 74	2525 ± 71
14′-COOH	405	13 ± 1	19 ± 1	26 ± 1	68 ± 1	1039 ± 49	1604 ± 69
10′-COOEt	450	12 ± 1	19 ± 1	22 ± 1	95 ± 3	542 ± 18	1287 ± 65
14′-COOMe	405	7 ± 0	13 ± 1	12 ± 1	62 ± 3	650 ± 74	941 ± 24
10′-CH_2OH	425	9 ± 1	20 ± 1	32 ± 2	95 ± 1	392 ± 19	1075 ± 27
14′-CH_2OH	371	10 ± 1	17 ± 1	29 ± 3	84 ± 0	377 ± 18	763 ± 26

[a] In micellar solution. [b] $n = 2$. [c] Estimated by graphical determination from the A(234 nm) *vs.* time curves recorded in the presence of both $MbFe^{III}$ and linoleic acid. For a given antioxidant, the same time interval is considered in the control experiments. [d] Period of time needed to consume half the initial antioxidant concentration in the presence of both $MbFe^{III}$ and linoleic acid.

not in accordance with the weaker antioxidant activity of apo-lycopenols compared to the other apo-lycopenoids (Fig. 4 and Table 3). It also does not reflect the higher potency of apo-lycopenoic acids. For data interpretation, ionisation potentials are thus of limited value and other criteria must also be considered, among which the partition of antioxidants between the lipid phase, interface and aqueous phase (including possible binding to metmyoglobin and its activated forms involved in the initiation of lipid peroxidation). Hence, log P values (P: *n*-octanol/water partition coefficient) were calculated to assess the relative affinity of lycopene and its derivatives for the lipid *vs.* aqueous phase (Table 3). As expected, the log P values of aldehydes on the one hand and esters on the other hand increase with the hydrocarbon chain length. As their antioxidant potency concomitantly increases, it can be suggested that these compounds act within the lipid phase by scavenging lipid-derived radicals. A similar correlation does not hold for alcohols and acids. In particular, **10′-COOH** and **14′-COOH** are equally potent at inhibiting lipid peroxidation while the former is much more lipophilic (higher log P) than the latter. This is also true for **10′-CH_2OH** and **14′-CH_2OH**. It can thus be suggested that the relative antioxidant efficiency of **14′-COOH**

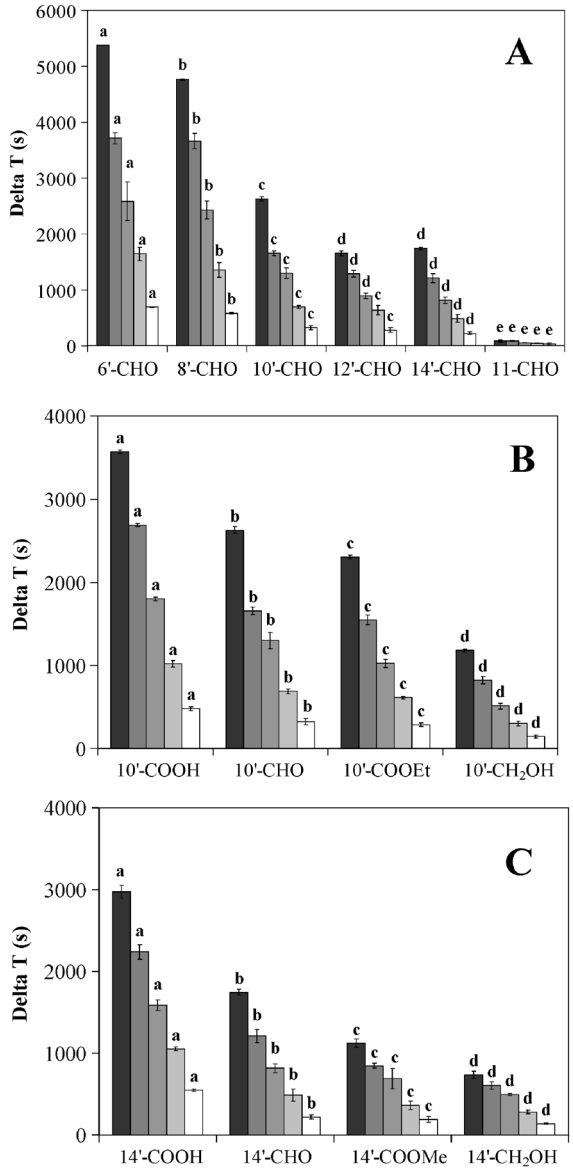

Fig. 4 Antioxidant activity of apo-lycopenoids in metmyoglobin-induced peroxidation of linoleic acid. For the same concentration, different letters point to significant differences between apo-lycopenoids (ANOVA, *post-hoc* S–N–K, $p < 0.05$). (A) Inhibition by apo-lycopenals. (B) Inhibition by apo-10′-lycopenoids. (C) Inhibition by apo-14′-lycopenoids. From black to white bars, antioxidant concentrations are: 10, 8, 6, 4, and 2 μM.

(and to a lesser degree **14′ CH_2OH**) reflects a specific protecting mechanism (see below).

Moreover, as an alternative to electron transfer, scavenging of the propagating lipid peroxyl radicals by addition of the latter to the polyene moiety of lycopene and apo-lycopenoids may occur as already demonstrated for β-carotene.[32] Hence, the energy changes for the addition of $MeOO^{\bullet}$ (a simple model for the peroxyl radicals derived from linoleic acid) to **10′-CH_2OH** and **10′-CHO** were estimated and plotted as a function of the site of addition (Fig. 5). The following comments can be made:

– The energy change is generally more exothermic with **10′-CHO** as a likely consequence of the extended delocalization in the radical adducts formed (participation of the aldehyde group in the conjugation). This difference is most pronounced for addition at C14′.

– Peroxyl addition is most favourable at C11′ (C-atom linked to the terminal group) because of maximal electron delocalization along the polyene chain. A similar situation occurs with addition at the other end (C5) but seems less favourable.

– Peroxyl addition is less favourable in the middle of the chain, especially when the C-atoms involved are methylated (C9, C13). It is also unfavourable at C6 and C12′ as conjugation in the corresponding radicals reaches a minimum.

The relatively unfavourable energy changes accompanying radical addition to **10′-CH_2OH** is consistent with its being a poorer antioxidant (despite being a better electron donor) than **10′-CHO** in our model.

In conclusion, there is a general trend toward more lipophilic apo-lycopenoids being better inhibitors of heme-induced lipid peroxidation in agreement with their higher affinity for micelles (higher log *P* value). As more lipophilic apo-lycopenoids also display a longer conjugated hydrocarbon chain, they are generally

Table 3 IC_{50} (inhibition of metmyoglobin-induced peroxidation of linoleic acid), I_p (ionisation potential) and log *P* (*P*: *n*-octanol/water partition coefficient) values of (all-*E*)-lycopene and the apo-lycopenoids investigated

Compounds	IC_{50}/μM[a]	$I_p = -E$(HOMO)/eV	log *P*
(all-*E*)-lyc.	1.94 ± 0.14	7.74	11.11
6′-CHO	0.94 ± 0.08	7.91	7.52
8′-CHO	1.27 ± 0.10	7.95	7.18
10′-CHO	2.35 ± 0.21	8.02	6.32
12′-CHO	3.21 ± 0.46	8.09	5.97
14′-CHO	3.47 ± 0.11	8.22	5.11
11-CHO	14.81 ± 1.57	8.81	3.39
10′-COOH	1.86 ± 0.24	8.04	6.58
14′-COOH	1.65 ± 0.09	8.25	5.37
11-COOH	20.11 ± 7.58	8.87	3.65
10′-COOEt	2.62 ± 0.15	8.02	7.18
14′-COOMe	3.41 ± 0.14	8.21	5.64
11-COOEt	27.10 ± 8.44	8.80	4.25
10′-CH_2OH	3.66 ± 0.35	7.84	6.62
14′-CH_2OH	3.61 ± 0.10	7.98	5.42
11-CH_2OH	11.41 ± 0.89	8.40	3.70

[a] Data are expressed as mean ± SD (n = 3–4).

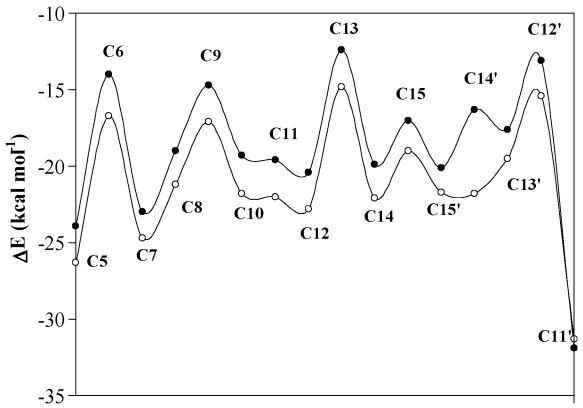

Fig. 5 Estimation of energy changes for the addition of $MeOO^{\bullet}$ (a simple model for the peroxyl radicals derived from linoleic acid) to **10′-CH_2OH** (full circles) and **10′-CHO** (empty circles) as a function of the site of addition on the unsaturated carbon chain (Catom number = C5 to C11′).

better electron donors. However, the favourable influence of terminal groups with an electron-withdrawing mesomeric effect (CHO, COOH, COOEt) *vs.* CH_2OH suggests that the antioxidant mechanism in micelles mainly proceeds *via* addition of the lipid peroxyl radicals on the polyene moiety of apo-lycopenoids (rather than electron transfer to the same radicals). The relative efficiency of short-chain apo-lycopenoids with polar terminal groups (mainly, **14′-COOH**) escapes those interpretations and has now to be further analyzed.

Reduction of hypervalent iron species derived from metmyoglobin. Our recent works[16,27,33] have shown that $MbFe^{III}$ efficiently initiates the peroxidation of LH in micelles by forming an ill-defined one-electron-oxidised form (simply noted $MbFe^{IV}$ for convenience) in its reaction with initial traces of lipid hydroperoxides (LOOH). $MbFe^{IV}$ can then react with a second LOOH molecule or a LH molecule to form the propagating lipid peroxyl radicals ($LOO^{\bullet}$). Depending on their hydrophilic–lipophilic balance, antioxidants were also shown to act as inhibitors of propagation (scavenging of $LOO^{\bullet}$ in the lipid phase) or inhibitors of initiation *via* reduction of $MbFe^{IV}$. The latter mechanism was in agreement with the ability of several water-soluble antioxidants to rapidly reduce ferrylmyoglobin ($MbFe^{IV}$=O).[16,33–35] Direct interaction between the heme crevice and anionic antioxidants like ascorbate and the polyphenol chlorogenic acid was also demonstrated.[36] Although probably different from $MbFe^{IV}$, ferrylmyoglobin will be taken as a model of the peroxidation-initiating species as this iron-oxo species has many advantages: it is relatively stable, conveniently detected in the visible range, and easily prepared by reacting $MbFe^{III}$ with H_2O_2. It was thus interesting to check whether some relatively polar apo-lycopenoids could reach the heme and reduce the iron-oxo centre, as already demonstrated in the case of the water-soluble carotenoid crocetin.[37] The reactions were run in the same conditions as those with linoleic acid *i.e.* in the presence of Tween 20.

When H_2O_2 (1 equiv.) is added to a solution of $MbFe^{III}$, this species is readily converted into $MbFe^{IV}$=O, which has a characteristic absorption band at 590 nm (Fig. 6A). After A(590 nm) reached a plateau, (all-*E*)-lycopene or apo-lycopenoids were added and changes in A(590 nm) were monitored. A significant decay was observed only after addition of **14′-COOH** (Fig. 6B), indicating that this sole derivative is able to reduce $MbFe^{IV}$=O back to $MbFe^{III}$. In particular, the other apo-14′-lycopenoids were inactive, thus showing that the carboxyl group is essential in this reaction. However, compared with quercetin, a potent flavonol antioxidant, **14′-COOH** appeared much less efficient (Fig. 7). From a fitting of the A(590 nm) *vs.* time curves relative to $MbFe^{IV}$=O formation from the equimolar mixture of $MbFe^{III}$ and H_2O_2, a value of $10^4\ M^{-1}\ cm^{-1}$ was obtained for the molar absorption coefficient of $MbFe^{IV}$=O (in good agreement with the literature[37]). This value was used for estimating the $MbFe^{IV}$=O and $MbFe^{III}$ concentrations at the time of antioxidant addition. An exponential fitting of the A(590 nm) *vs.* time curves obtained after addition of an antioxidant in excess gave apparent first-order rate constants (k_{obs}), from which second-order rate constants of ferrylmyoglobin reduction (k_r) were deduced: $k_{obs} = k_r C$ with C = initial antioxidant concentration. One obtained: k_r = 1150 (±210) and 7.7 (±1.1) $M^{-1}\ s^{-1}$ for quercetin and **14′-COOH**, respectively (37 °C, n = 2).

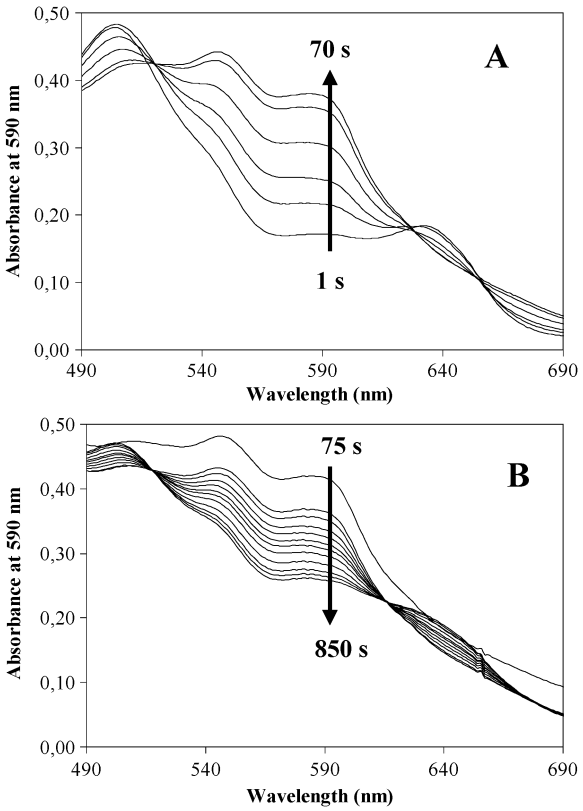

Fig. 6 (A) Spectral changes during the formation of ferrylmyoglobin. Metmyoglobin (100 μM) + H_2O_2 (100 μM), pH 7.4 phosphate buffer containing 2 mM Tween 20, 37 °C. (B) Spectral changes during reduction of ferrylmyoglobin by **14′-COOH** (300 μM).

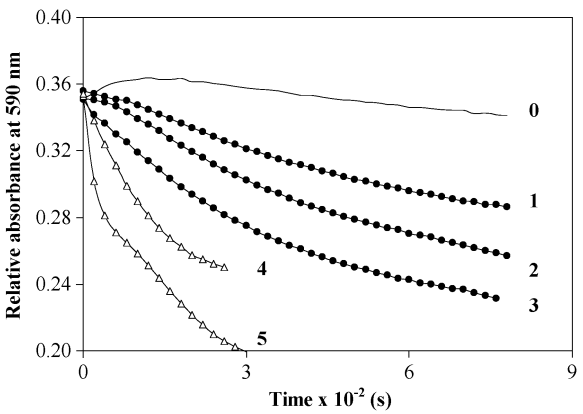

Fig. 7 Time dependence of the absorbance at 590 nm following the addition of **14′-COOH** (full circles, 100 μM: **1**, 200 μM: **2**, 300 μM: **3**) or quercetin (empty triangles, 100 μM: **4**, 200 μM: **5**) to a solution of ferrylmyoglobin (31–35 μM) in a pH 5.8 phosphate buffer containing 2 mM Tween 20, 37 °C. Control without antioxidant: **0**.

The value for quercetin can be compared with the one estimated at 10 °C in the absence of Tween 20: k_r = 280 $M^{-1}\ s^{-1}$.[38]

In a previous work,[16] we have shown that the inhibition of metmyoglobin-induced lipid peroxidation by quercetin essentially proceeds in the aqueous phase *via* a fast reduction of an activated iron species (distinct from ferrylmyoglobin) produced by reaction of metmyoglobin with the lipid hydroperoxides. We hypothesize that **14′-COOH** could act by a similar mechanism.

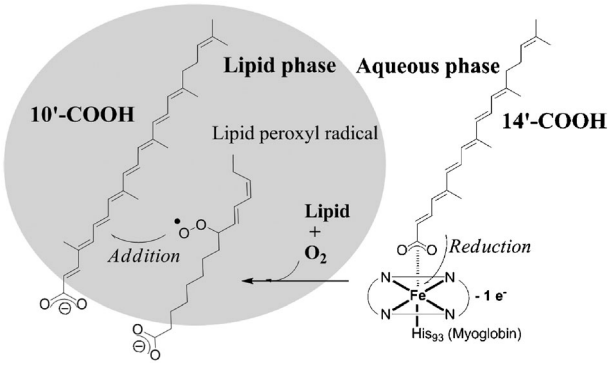

Scheme 3 Proposed mechanism for the inhibition of the metmyoglobin-induced peroxidation of linoleic acid by **10′-COOH** and **14′-COOH**.

In particular, **14′-COOH** could bind to the iron centre through its carboxylate group (Scheme 3). This hypothesis is comforted by the shape of the *A*(234 nm) *vs*. time curves recorded during the inhibition of lipid peroxidation by **14′-COOH**, which does not show a well-defined lag phase (Fig. 3A) as usually obtained for chain-breaking antioxidants acting in the lipid phase.[26] On the opposite, apo-lycopenoids with longer chains like **10′-COOH** and its analogues with different terminal groups must be too lipophilic to directly interact with activated metmyoglobin, thus staying in the lipid phase where they scavenge lipid peroxyl radicals (Scheme 3), as previously demonstrated for the typical chain-breaking antioxidant α-tocopherol.[16,27]

Conclusion

In this work, we demonstrated the ability of lycopene and apo-lycopenoids to inhibit the peroxidation of linoleic acid induced by heme iron in acidic micellar solutions. **6′-CHO**, which has the longest unsaturated chain among the apo-lycopenoids tested, was the best inhibitor, followed by **8′-CHO**. It is important to note that both long-chain apo-lycopenals, which have been evidenced in fresh tomato[39] and in tomato products,[20] are more antioxidant than lycopene itself in our model. For the same chain length, apo-lycopenoic acids come up as the most active molecules, which might be due to a more favourable hydrophilic/lipophilic balance allowing their location at the lipid–water interface. Both the chain length and terminal group of apo-lycopenoids thus govern their antioxidant activity and the mechanisms involved. In particular, **14′-COOH** behaves more as a hydrophilic antioxidant possibly reacting directly with hypervalent iron species in the aqueous phase whereas **10′-COOH**, its analogue with a longer chain, might exert its antioxidant action in the lipid phase by quenching lipid peroxyl radicals. Experiments are ongoing in our laboratory to better understand the different mechanisms involved in the antioxidant activity of apo-lycopenoids.

Experimental

Materials

(All-*E*)-lycopene, apo-8′-lycopenal and apo-12′-lycopenal were a gift from DSM (DSM Nutritional Products Ltd., Kaiseraugst, Switzerland). Pseudoionone was given by BASF (BASF Aktiengesellschaft, Ludwigshafen, Germany). Apo-6′-lycopenal was purchased from CaroteNature (CaroteNature GmbH, Lupsingen, Switzerland). Apo-10′-lycopenoic acid, ethyl apo-10′-lycopenoate, apo-14′-lycopenoic acid and methyl apo-14′-lycopenoate were obtained in our laboratory by multi-step organic synthesis.[25] Diisobutylaluminium hydride (DIBAH), manganese dioxide, ammonium formate, sylver oxide (Ag_2O), sodium hydride (NaH), 3 Å molecular sieves, horse heart metmyoglobin ($MbFe^{III}$, type II, MW *ca.* 17 600 g mol^{-1}), linoleic acid, quercetin and Tween 20 (polyoxyethylenesorbitan monolaurate) were purchased from Sigma-Aldrich (Sigma-Aldrich, Saint-Quentin Fallavier, France). Triethyl phosphonoacetate and benzophenone were purchased from Alfa Aesar (Alfa Aesar France, Schiltigheim, France). Buffer salts and all other chemicals were of analytical grade. The phosphate buffers (10 mmol, pH 5.8 or 6.8), prepared with grade water (18 MΩ) prepared using a Millipore Q-Plus water, were passed through a column of Chelex-100 chelating resin (Bio-Rad, Marnes-la-Coquette, France) to remove contaminating free metal ion traces. Silica gel (Si 60, 40–63 μm) was obtained from Merck (Merck France, Limonest, France). Celite was purchased from VWR (VWR International SAS, Fontenay sous Bois, France). Chloroform ($CHCl_3$) and methanol (MeOH) were of HPLC grade. All other solvents used were of analytical grade. The tetrahydrofurane (THF) used for chemical reactions was freshly distilled over Na–benzophenone. Ethyl acetate (AcOEt), ethanol, hexane, dichloromethane (CH_2Cl_2) and toluene were dried over 3 Å molecular sieves (previously dried at 150 °C for 4 h).

Analyses

HPLC-MS. HPLC-MS analyses were performed using a Hewlett Packard 1100 apparatus coupled to a UV/Vis diode array detector and a Micromass platform LCZ 4000 mass spectrometer. Mass analyses were performed in the positive electrospray ionization mode with a capillary voltage of 15 V and a desolvation temperature of 250 °C. The column used was a 150 mm × 2.1 mm i.d., 3 μm, YMC C30 column, with a 10 mm × 2 mm i.d. guard column of the same material (Interchim, Montluçon, France). The temperature of the column was set at 40 °C. The solvent system was a gradient of A (25 mmol ammonium formate + 2.6 mmol formic acid in water), B (25 mmol ammonium formate in MeOH) and C (methyl *tert*-butyl ether), with 60% B, 40% A at t = 0; 40% A, 60% B at t = 1.25 min; 30% A, 70% B at t = 2.50 min; 25% A, 70% B, 5% C at t = 3.75 min; 20% A, 70% B, 10% C at t = 5 min; 5% A, 10% B, 85% C at t = 15 min; and 5% A, 10% B, 85% C at t = 25 min (flow rate = 0.5 ml min^{-1}).

TLC. Analytical thin layer chromatography (TLC) was performed on silica gel plates (Merck Kieselgel 60 F_{254}) with UV detection at 254 or 365 nm.

GC-MS. Volatile products were monitored by GC-MS (CP2010; Shimadzu, Kyoto). Samples (1 μl) were injected onto a UBWAX 52 CB capillary column (30 m, 0.25 mm i.d., 0.5 μm thickness). The injection port was operated in split mode (R = 1/10). The carrier gas (He) velocity was constant (60 cm s^{-1}). The initial oven temperature of 60 °C was increased at a rate of 5 °C per min to 230 °C. This final temperature was maintained for 15 min. The mass spectrometer was operated in the electron

impact mode at 70 eV with continuous scans (every 0.5 s) in the range *m*/*z* 29–350. Data were analyzed using the GC-MS solution software.

NMR. ^{1}H and ^{13}C NMR spectra were recorded on a Bruker Advance DRX 500 MHz spectrometer. Chemical shifts are given in ppm relative to peak solvent ($CDCl_3$).[40] *J* values are given in Hz. Signal assignments were deduced from a combination of heteronuclear single quantum coherence (HSQC), distortionless enhancement by polarization transfer quantum (DEPTQ 135), nuclear overhauser effect spectroscopy (NOESY), correlation spectroscopy (COSY) and heteronuclear multiple bond coherence (HMBC) spectra.

HRMS. High-resolution mass analysis was carried out using a QStar Elite (Applied Biosystems SCIEX) with positive electrospray-TOF ionisation. High-resolution mass analysis was carried out on an Ultraflextreme TOF/TOF (Bruker) with NALDI™ ionisation for compound **14′-CH_2OH**.

Synthesis of apo-10′-, apo-14′- and apo-11-lycopenoids

All reactions were carried out under dim light and argon atmosphere.

Synthesis of apo-10′-lycopenoids

(2E,4E,6E,8E,10E,12E,14E,16E,20E)-4,9,13,17,21-Pentamethyldocosa-2,4,6,8,10,12,14,16,20-nonaen-1-ol (apo-10′-lycopenol, ***10′-CH_2OH***). Ethyl apo-10′-lycopenoate (**10′-COOEt**)[25] (287 mg, 0.68 mmol) was dissolved in dry THF (5 ml). A solution of DIBAH (1.7 mmol) in toluene (1.4 ml) was carefully added over 30 min at 0 °C. The mixture was stirred for 4 h, then a MeOH/water (3 ml, 1/1, v/v) mixture was slowly added at 0 °C. The gel formed was destroyed by addition of a 2 M potassium sodium tartrate aqueous solution (10 ml) and vigorous stirring for 10 h. Then, the product was extracted with diethylether (3 × 10 ml). The combined organic phases were dried over Na_2SO_4 and concentrated. The crude product was purified by filtration through a silica gel chromatographic column (eluent hexane/AcOEt (1/1, v/v)), then crystallized from CH_2Cl_2/hexane. Compound **10′-CH_2OH** was obtained as a red powder (80 mg, 31%).

δ_H (500 MHz; $CDCl_3$) 1.39 (1H, t, *J* 5.85, OH), 1.61 (3H, s, C(21)Me), 1.69 (3H, s, C(22) H_3), 1.82 (3H, s, C(17)Me), 1.91 (3H, s, C(4)Me), 1.97 (6H, s, C(9, 13)Me), 2.12 (4H, m, C(18, 19) H_2), 4.25 (2H, t, *J* 6.1, C(1)H), 5.11 (1H, m, C(20)H), 5.88 (1H, dt, *J* 6.1 and 15.6, C(2)H), 5.95 (1H, d, *J* 11.0, C(16)H), 6.18 (1H, d, *J* 11.5, C(12)H), 6.21 (1H, d, *J* 11.5, C(8)H), 6.23 (1H, d, *J* 11.0, C(5)H), 6.25 (1H, d, *J* 15.2, C(14)H), 6.34 (1H, d, *J* 15.6, C(3)H), 6.35 (1H, d, *J* 15.0, C(10)H), 6.49 (1H, dd, *J* 11.0 and 15.2, C(15)H), 6.59 (1H, m, C(6)H), 6.61 (1H, m, C(7)H), 6.64 (1H, m, C(11)H).

δ_C (125 MHz; $CDCl_3$) 13.0 (C(4)Me), 13.0 (C(9)Me), 13.0 (C(13)Me), 17.1 (C(17)Me), 17.9 (C(21)Me), 25.9 (C(22)), 26.8 (C(19)), 40.4 (C(18)), 64.1 (C(1)), 124.1 (C(20)), 125.0 (C(15)), 125.5 (C(11)), 125.9 (C(16)), 127.5 (C(2)), 129.6 (C(6)), 130.6 (C(7)), 131.6 (C(12)), 131.9 (C(21)), 132.4 (C(8)), 132.5 (C(5)), 134.9 (C(4)), 135.5 (C(14)), 136.4 (C(13)), 136.5 (C(3)), 136.9 (C(9)), 137.4 (C(10)), 139.7 (C(17)).

HRMS: *m*/*z* 379.2978 ($[M + H]^+$) (379.2995 calculated for $C_{27}H_{39}O$).

HPLC-UV/Vis-MS: t_R 13.02 min; λ_{max}/nm 396, <u>418</u>, 444 (main absorption band is underlined), *m*/*z* 379.5 ($[M + H]^+$), 361.5 ($[M + H]^+$-H_2O).

(2E,4E,6E,8E,10E,12E,14E,16E,20E)-4,9,13,17,21-Pentamethyldocosa-2,4,6,8,10,12,14,16,20-nonaenal (apo-10′-lycopenal, ***10′-CHO***). Compound **10′-CH_2OH** (90 mg, 0.24 mmol) was dissolved in AcOEt (5 ml). After addition of MnO_2 (510 mg, 5 mmol), the heterogeneous mixture was vigorously stirred at room temperature for 2 h. Then, the mixture was filtered off through Celite, dried over Na_2SO_4 and concentrated. The residue was purified by filtration through a silica gel chromatographic column (eluent hexane/AcOEt (2/8, v/v)). Compound **10′-CHO** was obtained as a red powder (40 mg, 44%).

δ_H (500 MHz; $CDCl_3$) 1.61 (3H, s, C(21)Me), 1.69 (3H, s, C(22)H_3), 1.82 (3H, s, C(17)Me), 1.96 (3H, s, C(4)Me), 1.98 (3H, s, C(13)Me), 2.01 (3H, s, C(9)Me), 2.12 (4H, m, C(18, 19)H_2), 5.11 (1H, m, C(20)H), 5.95 (1H, d, *J* 11.0, C(16)H), 6.18 (1H, dd, *J* 7.8 and 15.3, C(2)H), 6.18 (1H, d, *J* 11.6, C(12)H), 6.25 (1H, d, *J* 15.1, C(14)H), 6.28 (1H, d, *J* 12.1, C(8)H), 6.36 (1H, d, *J* 14.9, C(10)H), 6.53 (1H, dd, *J* 11.0 and 15.1, C(15)H), 6.61 (1H, m, C(6)H), 6.61 (1H, m, C(5)H), 6.73 (1H, dd, *J* 11.6 and 14.9, C(11)H), 6.86 (1H, m, C(7)H), 7.15 (1H, d, *J* 15.3, C(3)H), 9.58 (1H, d, *J* 7.8, C(1)H).

δ_C (125 MHz; $CDCl_3$) 12.9 (C(4)Me), 13.1 (C(9)Me), 13.1 (C(13)Me), 17.1 (C(17)Me), 17.8 (C(21)Me), 25.8 (C(22)), 26.8 (C(19)), 40.4 (C(18)), 124.0 (C(20)), 125.7 (C(15)), 125.8 (C(16)), 127.2 (C(2)), 127.2 (C(11)), 128.6 (C(6)), 131.3 (C(12)), 131.7 (C(8)), 131.8 (C(21)), 133.8 (C(4)), 135.3 (C(14)), 135.5 (C(7)), 136.8 (C(10)), 137.7 (C(13)), 140.2 (C(9)), 140.3 (C(17)), 141.3 (C(5)), 156.7 (C(3)), 193.8 (C(1)).

HRMS: *m*/*z* 377.2823 ($[M + H]^+$) (377.2839 calculated for $C_{27}H_{37}O$).

HPLC-UV/Vis-MS: t_R 13.61 min, λ_{max}/nm 458, *m*/*z* 377.5 ($[M + H]^+$).

Synthesis of apo-14′-lycopenoids

(2E,4E,6E,8E,10E,12E,16E)-5,9,13,17-Tetramethyloctadeca-2,4,6,8,10,12,16-heptaen-1-ol (apo-14′-lycopenol, ***14′-CH_2OH***). A solution of DIBAH (3.5 mmol) in toluene (3.5 ml) was carefully added over 1 h to a solution of methyl apo-14′-lycopenoate (**14′-COOMe**)[25] (500 mg, 1.47 mmol) in dry THF (20 ml) at 0 °C and the resulting mixture stirred for 3 h at 0 °C. The reaction was quenched by careful addition of MeOH/water (5 ml, 1/1, v/v) at 0 °C. The gel thus formed was dissociated by addition of aqueous 2 M potassium sodium tartrate (20 ml) and vigorous stirring for 10 h. Then, the product was extracted with diethylether (3 × 10 ml) and the combined organic phases dried over Na_2SO_4 and concentrated. The residue was purified by filtration through a silica gel chromatographic column (eluent hexane/AcOEt (1/1, v/v)), then crystallized from CH_2Cl_2/hexane. Compound **14′-CH_2OH** was obtained as an orange powder (163 mg, 35%).

δ_H (500 MHz; $CDCl_3$) 1.4 (1H, t, *J* 5.8, HO), 1.61 (3H, s, C(17)Me), 1.69 (3H, s, C(18)H_3), 1.82 (3H, s, C(13)Me), 1.94 (3H, s, C(5)Me), 1.95 (3H, s, C(9)Me), 2.12 (4H, m, C(14, 15)H_2), 4.25 (2H, t, *J* 5.9, C(1)H_2), 5.11 (1H, m, C(16)H), 5.89 (1H, dt, *J* 5.9 and 14.9, C(2)H), 5.95 (1H, d, *J* 11.0, C(12)H), 6.12 (1H, d, *J* 11.4, C(4)H), 6.16 (1H, d, *J* 11.4, C(8)H),

6.24 (1H, d, *J* 15.0, C(10)H), 6.31 (1H, d, *J* 14.9, C(6)H), 6.49 (1H, dd, *J* 11.0 and 15, C(11)H), 6.63 (2H, m, C(3, 7)H).

δ_C (125 MHz; $CDCl_3$) 12.8 (C(5)Me), 13.0 (C(9)Me), 17.1 (C(13)Me), 17.8 (C(17)Me), 25.8 (C(18)), 26.8 (C(15)), 40.4 (C(14)), 63.9 (C(1)), 124.1 (C(16)), 125.1 (C(11)), 125.7 (C(7)), 125.8 (C(12)), 128.4 (C(3)), 130.5 (C(8)), 131.1 (C(17)), 131.3 (C(4)), 132.4 (C(2)), 135.4 (C10)), 136.4 (C(9)), 136.7 (C(5)), 137.1 (C(6)), 139.7 (C(13)).

HRMS (For **14′-CH_2OH** high-resolution mass analysis was carried out on an Ultraflextreme TOF/TOF (Bruker) with NALDI™ ionisation): *m*/*z* 312.2441 $[M]^+$ (312.2448 calculated for $C_{22}H_{32}O$).

HPLC-UV/Vis-MS: t_R 11.28 min, λ_{max}/nm 348, 366, 387, *m*/*z* 313.3 ($[M + H]^+$), 295.2 ($[M + H]^+$-H_2O).

(2E,4E,6E,8E,10E,12E,16E)-5,9,13,17-Tetramethyloctadeca-2,4,6,8,10,12,16-heptaenal (apo-14′-lycopenal, ***14′-CHO***). MnO_2 (175 mg, 2 mmol) was added to a solution of **14′-CH_2OH** (26 mg, 0.08 mmol) in AcOEt (1 ml). The heterogeneous mixture was vigorously stirred at room temperature for 1 h, then filtered off through Celite, dried over Na_2SO_4 and concentrated. The residue was purified by filtration through a silica gel chromatographic column (eluent hexane/AcOEt (2/8, v/v)). Compound **14′-CHO** was obtained as an orange powder (11 mg, 44%).

δ_H (500 MHz; $CDCl_3$) 1.62 (3H, s, C(17)Me), 1.69 (3H, s, C(18)H_3), 1.83 (3H, s, C(13)Me), 2 (3H, s, C(9)Me), 2.11 (3H, s, C(5)Me), 2.12 (4H, m, C(14, 15)H_2), 5.11 (1H, m, C(16)H), 5.96 (1H, d, *J* 11.1, C(12)H), 6.17 (1H, dd, *J* 7.9 and 14.8, C(2)H), 6.20 (1H, d, *J* 11.5, C(8)H), 6.26 (1H, d, *J* 15.0, C(10)H), 6.35 (1H, d, *J* 11.9, C(4)H), 6.38 (1H, d, *J* 15.0, C(6)H), 6.59 (1H, dd, *J* 11.1 and 15, C(11)H), 6.91 (1H, dd, *J* 11.5 and 15, C(7)H), 7.52 (1H, dd, *J* 11.8 and 14.8, C(3)H), 9.61 (1H, d, *J* 8.0, C(1)H).

δ_C (125 MHz; $CDCl_3$) 13.3 (C(9)Me), 13.6 (C(5)Me), 17.2 (C(13)Me), 17.8 (C(17)Me), 25.8 (C(18)), 26.8 (C(15)), 40.4 (C(14)), 124.0 (C(16)), 125.7 (C(12)), 126.8 (C(11)), 128.7 (C(4)), 130.1 (C(7)), 130.7 (C(8)), 130.9 (C(2)), 132 (C(17)), 135 (C10)), 135.7 (C(6)), 139.8 (C(9)), 141.2 (C(13)), 146.8 (C(5)), 147.7 (C(3)), 193.7 (C(1)).

HRMS: *m*/*z* 311.2369 ($[M + H]^+$) (311.2369 calculated for $C_{22}H_{31}O$).

HPLC-UV/Vis-MS: t_R 13.61 min, λ_{max}/nm 422, *m*/*z* 311.5 ($[M + H]^+$).

Synthesis of apo-11-lycopenoids

Ethyl (2E and 2Z,4E,6E)-3,7,11-trimethyldodeca-2,4,6,10-tetraenoate (ethyl apo-11-lycopenoate, ***11-COOEt***). Triethyl phosphonoacetate (10 ml, 49 mmol) was slowly added at 0 °C in a heterogenous mixture containing 30 ml of dry THF and NaH (1.96 mg, 48 mmol) previously washed with hexane (3 × 20 ml). After the end of hydrogen release, pseudoionone (**PI**, 2.2 ml, 9.8 mmol) was added over 1 h then the mixture stirred for 30 h at room temperature. The reaction was then quenched with 25 ml of saturated aqueous NH_4Cl solution and the product extracted with diethylether (3 × 10 ml). The combined organic layers were washed with brine (3 × 10 ml), dried over Na_2SO_4 and concentrated. The residue was purified on silica gel (eluent EtOAc/hexane (2/98, v/v)) to afford compound **11-COOEt** as a light-yellow oil (2.1 g, 82%, (*E*/*Z*) = 3.5 (determined by HPLC)).

δ_H (500 MHz; $CDCl_3$) 1.29 (3H, t, *J* 7.1, CH_2CH_3), 1.61 (3H, s, C(11)Me), 1.69 (3H, s, C(12)H_3), 1.85 (3H, s, C(7)Me), 2.13 (4H, m, C(8, 9)H_2), 2.32 (3H, s, C(3)Me), 4.16 (2H, q, *J* 7.1, CH_2CH_3), 5.09 (1H, m, C(10)H), 5.62 (1H, s, C(2*Z*)H), 5.74 (1H, s, C(2*E*)H), 5.96 (1H, d, *J* 11.1, C(6)H), 6.18 (1H, d, *J* 15.3, C(4)H), 6.84 (1H, dd, *J* 11.1 and 15.3, C(3)H).

δ_C (125 MHz; $CDCl_3$) 14.1 (C(3)Me), 14.9 (CH_2CH_3), 17.4 (Me-C(7)), 18.2 (Me-C(11)), 26.4 (C(12)), 27.0 (C(9)), 40.8 (C(8)), 59.9 (CH_2CH_3), 116.5 (C(2*Z*)), 118.4 (C(2*E*)), 123.9 (C(10)), 125.2 (C(6)), 131.5 (C(5)), 132.2 (C(11)), 133.6 (C(4)), 144.1 (C7)), 153.2 (C(3)), 167.3 (C(1)).

HRMS: *m*/*z* 263.2003 ($[M + H]^+$) (263.2005 calculated for $C_{17}H_{27}O_2$).

HPLC-UV/Vis-MS: $t_{R(2Z)}$ 9.76 min and $t_{R(2E)}$ 10.40 min, λ_{max}/nm 318, *m*/*z* 263.2 ($[M + H]^+$). GC-MS: $t_{R(2Z)}$ 34.3 min and $t_{R(2E)}$ 34.9 min, *m*/*z* 262 (M^+).

(2E,4E,6E)-3,7,11-Trimethyldodeca-2,4,6,10-tetraen-1-ol (apo-11-lycopenol, ***11-CH_2OH***). A solution of DIBAH (1.9 mmol) in hexane (1.9 ml) was carefully added over 1 h to a solution of **11-COOEt** (210 mg, 0.75 mmol) in dry THF (5 ml) at 0 °C and the resulting mixture stirred for 3 h at room temperature. The reaction was quenched by careful addition of MeOH/water (5 ml, 1/1, v/v) at 0 °C. The gel thus formed was dissociated by addition of aqueous 2 M potassium sodium tartrate (20 ml) and vigorous stirring for 10 h. Then, the product was extracted with diethylether (3 × 10 ml) and the combined organic phases dried over Na_2SO_4 and concentrated. The residue was purified and diastereoisomers were separated by an open silica gel chromatographic column (eluent hexane/AcOEt (8/2, v/v)). Compound **11-CH_2OH** was obtained as a white solid (27 mg, 16%).

δ_H (500 MHz; $CDCl_3$) 1.61 (3H, s, C(11)Me), 1.69 (3H, s, C(12)H_3), 1.79 (3H, s, C(3)Me), 1.83 (3H, s, C(7)Me), 2.11 (4H, m, C(8, 9)H_2), 4.27 (2H, d, *J* 7.0, C(1)H_2), 5.10 (1H, m, H-C(10)), 5.63 (1H, t, *J* 7, C(2)H), 5.9 (1H, d, *J* 10.8, C(6)H), 6.17 (1H, d, *J* 15.3, C(4)H), 6.46 (1H, dd, *J* 10.8 and 15.3, C(5)H).

δ_C (125 MHz; $CDCl_3$) 12.6 (C(3)Me), 16.8 (C(7)Me), 17.6 (C(11)Me), 25.6 (C(12)), 26.6 (C(9)), 40.1 (C(8)), 59.4 (C(1)), 123.9 (C(10)), 125.0 (C(5)), 125.2 (C(6)), 129.0 (C(2)), 131.7 (C(11)), 134.3 (C4)), 136.9 (C(3)), 139.6 (C(7)).

HRMS: *m*/*z* 243.1717 ($[M + Na]^+$) (243.1719 calculated for $C_{15}H_{24}ONa$).

HPLC-UV/Vis-MS: t_R 7.79 min, λ_{max}/nm 279, *m*/*z* 203.1 ($[M + H]^+$-H_2O).

(2E,4E,6E)-3,7,11-Trimethyldodeca-2,4,6,10-tetraenal (apo-11-lycopenal, ***11-CHO***). MnO_2 (14 g, 140 mmol) was added to a solution of diastereoisomeric mixture of **11-CH_2OH** (1.37 g, 6.2 mmol) in AcOEt (25 ml). The heterogeneous mixture was vigorously stirred at room temperature for 3 h, then filtered off through Celite, dried over Na_2SO_4 and concentrated. The residue was purified and diastereoisomers were separated by an open silica gel chromatographic column (eluent hexane/AcOEt (9/1, v/v)). Compound **11-CHO** was obtained as a light-yellow oil (400 mg, 30%).

δ_H (500 MHz; $CDCl_3$) 1.61 (3H, s, C(11)Me), 1.69 (3H, s, C(12)H_3), 1.87 (3H, s, C(7)Me), 2.14 (4H, m, C(8, 9)H_2),

2.30 (3H, s, C(3)Me), 5.09 (1H, m, C(10)H), 5.95 (1H, d, *J* 8, C(2)H), 6.01 (1H, d, *J* 11.1, C(6)H), 6.26 (1H, d, *J* 15.3, C(4)H), 6.99 (1H, dd, *J* 11.1 and 15.3, C(5)H), 10.10 (1H, d, *J* 8.0, C(1)H).

δ_C (125 MHz; $CDCl_3$) 13.7 (C(3)Me), 17.7 (C(7)Me), 18.3 (C(11)Me), 26.2 (C(12)), 26.9 (C(9)), 40.7 (C(8)), 123.7 (C(10)), 125.2 (C(6)), 129.1 (C(2)), 132.4 (C(11)), 132.9 (C(5)), 133.3 (C4)), 146.5 (C(7)), 155.3 (C(3)), 191.6 (C(1)).

HRMS: *m*/*z* 241.1563 ($[M + Na]^+$) (241.1562 calculated for $C_{15}H_{22}ONa$).

HPLC-UV/Vis-MS: t_R 7.90 min, λ_{max}/nm 344, *m*/*z* 219.0 ($[M + H]^+$).

(2E,4E,6E)-3,7,11-Trimethyldodeca-2,4,6,10-tetraenoic acid (apo-11-lycopenoic acid, ***11-COOH****)*. Ag_2O (3.7 g, 26 mmol) and NaOH (230 mg, 5.3 mmol) dissolved in EtOH (20 ml) were added to a solution of **11-CHO** (230 mg, 1.1 mmol) in toluene (20 ml). The heterogeneous mixture was vigorously stirred at room temperature for 20 h, then filtered off through Celite. The filtrate was washed with diluted HCl solution (3 × 10 ml) then dried over Na_2SO_4 and the solvent removed under vacuum. Compound **11-COOH** was obtained as an amorphous yellow solid (221 mg, 90%).

δ_H (500 MHz; $CDCl_3$) 1.61 (3H, s, C(11)Me), 1.69 (3H, s, C(12)H_3), 1.85 (3H, s, C(7)Me), 2.13 (4H, m, C(8, 9)H_2), 2.34 (3H, s, C(3)Me), 5.09 (1H, m, C(10)H), 5.77 (1H, s, C(2)H), 5.98 (1H, d, *J* 10.9, C(6)H), 6.21 (1H, d, *J* 15.1, C(4)H), 6.90 (1H, dd, *J* 10.9 and 15.1, C(5)H).

δ_C (125 MHz; $CDCl_3$) 14.2 (C(3)Me), 17.4 (C(7)Me), 17.9 (C(11)Me), 25.9 (C(12)), 26.6 (C(9)), 40.4 (C(8)), 117.1 (C(2)), 123.7 (C(10)), 125.0 (C(6)), 132.2 (C(5)), 132.2 (C(11)), 133.4 (C4)), 145.0 (C(7)), 155.9 (C(3)), 172.0 (C(1)).

HRMS: *m*/*z* 257.1515 ($[M + Na]^+$) (257.1512 calculated for $C_{15}H_{22}O_2Na$).

HPLC-UV/Vis-MS: t_R 5.83 min, λ_{max}/nm 301, *m*/*z* 235.3 ($[M + H]^+$).

Kinetic experiments

All kinetic experiments were recorded by UV-visible spectroscopy on a SPECORD® diode-array spectrometer (Analytik Jena, Germany) or on a Hewlett-Packard 8453 diode-array spectrometer (Agilent Technologies, France). Solutions in cells (optical pathlength: 1 cm) were stirred with a magnetic stirrer and thermostated at 37 (±1) °C.

Inhibition of the metmyoglobin-induced peroxidation of linoleic acid

The experimental conditions used were adapted from already published procedures.[15] Metmyoglobin ($MbFe^{III}$, 17.6 mg) was dissolved in 50 ml of phosphate buffer (10 mM, pH 6.8). Its concentration was standardized at 10 μM using ε = 7700 M^{-1} cm^{-1} at 525 nm.[41] Given volumes of daily prepared solutions of linoleic acid (7 mM), Tween 20 (40 mM), (all-*E*)-lycopene and apo-lycopenoids (1 mM) in $CHCl_3$ were mixed and the solvent removed under reduced pressure in darkness and 25 °C. The residue was dissolved immediately in 20 ml of 10 mM phosphate buffer at pH 5.8 under gentle stirring. The final concentrations in the solution were: linoleic acid, 0.7 mM; Tween 20, 2 mM; (all-*E*)-lycopene, 0.5–2.5 μM and apo-lycopenoids, 0.5–10 μM. Two ml of the freshly prepared solution were transferred to the spectrometer cells. At time zero, lipid oxidation was initiated by adding 20 μl of the metmyoglobin solution (final concentration in cell: 100 nM). The UV-visible spectra were recorded at regular time intervals (26 s). Each experiment was repeated three or four times at different antioxidant concentrations.

Stability of (all-*E*)-lycopene and apo-lycopenoids

The same experimental conditions were used to estimate the stability of (all-*E*)-lycopene (2 μM) and apo-lycopenoids (10 μM) without linoleic acid or metmyoglobin or both. The UV-visible spectra were recorded at regular time intervals (5 s). Each experiment was duplicated at different antioxidant concentrations.

Reduction of ferrylmyoglobin

Ferrylmyoglobin ($MbFe^{IV}$=O) was previously formed in the spectrometer cell by adding 20 μl of a 5 mM aqueous solution of H_2O_2 (concentration determined using ε = 39.4 M^{-1} cm^{-1} at 240 nm, final concentration in the cell: 100 μM) to 1 ml of a 100 μM $MbFe^{III}$ solution in 10 mM phosphate buffer containing 2 mM Tween 20 (pH 7.4). The spectral changes featuring the conversion of $MbFe^{III}$ into $MbFe^{IV}$=O were recorded in the visible range until stability (2–3 minutes). Then, 1 ml of a concentrated solution of an antioxidant (apo-lycopenoids or quercetin) in the same phosphate buffer–Tween 20 solution was added in the cell (final concentrations: 100, 200 and 300 μM) and the reduction of $MbFe^{IV}$=O back to $MbFe^{III}$ was monitored at 590 nm. Each experiment was duplicated at different antioxidant concentrations.

Data analysis and semi-empirical quantum mechanics calculations

Curve-fittings were carried out on a PC using the Scientist program (MicroMath, Salt Lake City, USA). Differences of antioxidant activity between (all-*E*)-lycopene and apo-lycopenoids were tested for significance by a one-way ANOVA procedure using Student–Newman–Keuls *post-hoc* test (XLSTAT for Microsoft Excel version 2009.2.04). Differences were considered to be significant at $p < 0.05$.

Semi-empirical quantum mechanics calculations were run on the HyperChem 5.1 software (Hypercube, Waterloo, Canada). HOMO energies were calculated using the PM3 program. Energy changes for radical addition (difference between the energy of adduct and the sum of the energies of starting polyene and methylperoxyl radical) were calculated using the AM1 program (UHF mode).

Values of log *P* (*P*: *n*-octanol/water partition coefficient) were calculated using the ChemPro program (ChemDraw Pro 11.0 CambridgeSoft).

Acknowledgements

This work was supported by a grant from the European Community's Sixth Framework Program (Lycocard, Integrated European Project No. 016213). Special thanks are given to Bettina Wüstenberg and Werner Simon (DSM Nutritional Products Ltd., Kaiseraugst, Switzerland) for their generous gift

of (all-*E*)-lycopene, apo-8′-lycopenal and apo-12′-lycopenal and to Hansgeorg Ernst (BASF Aktiengesellschaft, Fine Chemicals, and Biocatalysis Research, Ludwigshafen, Germany) for his generous gift of pseudoionone. We thank Claude Marfisi (LEA/Bruker) for the HRMS analysis of **14′-CH_2OH**. We also thank Christian Giniès for his help with GC-MS analyses and the Spectropole in Marseille for their assistance in NMR and HRMS analyses.

Notes and references

1 A. V. R. Rao and S. Agarwal, *J. Am. Coll. Nutr.*, 2000, **19**, 563–569.
2 H. D. Sesso, S. M. Liu, J. M. Gaziano and J. E. Buring, *J. Nutr.*, 2003, **133**, 2336–2341.
3 H. D. Sesso, J. E. Buring, E. P. Norkus and J. M. Gaziano, *Am. J. Clin. Nutr.*, 2004, **79**, 47–53.
4 E. Giovannucci, *J. Nutr.*, 2005, **135**, 2030S–2031S.
5 G. Britton, S. Liaaen-Jensen and H. Pfander, *Carotenoids Handbook*, Birkhaüser, 2004, pp. 563.
6 B. L. Lindshield, K. Canene-Adams and J. W. Erdman, *Arch. Biochem. Biophys.*, 2007, **458**, 136–140.
7 A. J. Young and G. M. Lowe, *Arch. Biochem. Biophys.*, 2001, **385**, 20–27.
8 W. Stahl and H. Sies, *Mol. Aspects Med.*, 2003, **24**, 345–351.
9 P. Di Mascio, S. Kaiser and H. Sies, *Arch. Biochem. Biophys.*, 1989, **274**, 532–538.
10 N. I. Krinsky and E. J. Johnson, *Mol. Aspects Med.*, 2005, **26**, 459–516.
11 V. L. Freeman, M. Meydani, S. Yong, J. Pyle, Y. Wan, R. Arvizu-Durazo and Y. Liao, *Am. J. Epidemiol.*, 2000, **151**, 109–118.
12 V. Tyssandier, E. Reboul, J. F. Dumas, C. Bougteloup-Demange, M. Armand, J. Marcand, M. Sallas and P. Borel, *Am. J. Physiol.: Gastrointest. Liver Physiol.*, 2003, **284**, G913–G923.
13 J. Kanner and T. Lapidot, *Free Radical Biol. Med.*, 2001, **31**, 1388–1395.
14 B. Halliwell, K. Zhao and M. Whiteman, *Free Radical Res.*, 2001, **33**, 819–830.
15 J. S. Cohn, *Curr. Opin. Lipidol.*, 2002, **13**, 19–24.
16 E. Vulcain, P. Goupy, C. Caris-Veyrat and O. Dangles, *Free Radical Res.*, 2005, **39**, 547–563.
17 J. W. Erdman, N. A. Ford and B. L. Lindshield, *Arch. Biochem. Biophys.*, 2009, **483**, 229–235.
18 M. Gajic, S. Zaripheh, F. R. Sun and J. W. Erdman, *J. Nutr.*, 2006, **136**, 1552–1557.
19 K. Q. Hu, C. Liu, H. Ernst, N. I. Krinsky, R. M. Russell and X. D. Wang, *J. Biol. Chem.*, 2006, **281**, 19327–19338.
20 R. E. Kopec, K. M. Riedl, E. H. Harrison, R. W. Curley, D. P. Hruszkewycz, S. K. Clinton and S. J. Schwartz, *J. Agric. Food Chem.*, 2010, **58**, 3290–3296.
21 W. Stahl, J. von Laar, H.-D. Martin, T. Emmerich and H. Sies, *Arch. Biochem. Biophys.*, 2000, **373**, 271–274.
22 F. Lian and X. D. Wang, *Int. J. Cancer*, 2008, **123**, 1262–1268.
23 K. Linnewiel, H. Ernst, C. Caris-Veyrat, A. Ben-Dor, A. Kampf, H. Salman, M. Danilenko, J. Levy and Y. Sharoni, *Free Radical Biol. Med.*, 2009, **47**, 659–667.
24 A. Ben-Dor, M. Steiner, L. Gheber, M. Danilenko, N. Dubi, K. Linnewiel, A. Zick, Y. Sharoni and J. Levy, *Mol. Cancer Ther.*, 2005, **4**, 177–186.
25 E. Reynaud, G. Aydemir, R. Rühl, O. Dangles and C. Caris-Veyrat, *J. Agric. Food Chem.*, 2011, **59**, 1457–1463.
26 J. R. Mein, F. Lian and X. D. Wang, *Nutr. Rev.*, 2008, **66**, 667–683.
27 P. Goupy, E. Vulcain, C. Caris-Veyrat and O. Dangles, *Free Radical Biol. Med.*, 2007, **43**, 933–946.
28 P. Goupy, A. B. Bautista-Ortin, H. Fulcrand and O. Dangles, *J. Agric. Food Chem.*, 2009, **57**, 5762–5770.
29 C. Caris-Veyrat, A. Schmid, M. Carail and V. Böhm, *J. Agric. Food Chem.*, 2003, **51**, 7318–7325.
30 G. Britton, in *Carotenoids. Volume 1B: Spectroscopy*, ed. G. Britton, S. Liaaen-Jensen and H. Pfander, Birkhäuser Verlag, 1995, vol. 1B, pp. 13–62.
31 J. R. Mancuso, D. J. McClements and E. A. Decker, *J. Agric. Food Chem.*, 1999, **47**, 4146–4149.
32 D. C. Liebler and T. D. McClure, *Chem. Res. Toxicol.*, 1996, **9**, 8–11.
33 B. Lorrain, C. Dufour and O. Dangles, *Free Radical Biol. Med.*, 2010, **48**, 1162–1172.
34 C. P. Baron and H. J. Andersen, *J. Agric. Food Chem.*, 2002, **50**, 3887–3897.
35 C. U. Carlsen, J. S. K. Møller and L. H. Skibsted, *Coord. Chem. Rev.*, 2005, **249**, 485–498.
36 C. U. Carlsen, M. V. Kroger-Ohlsen, R. Bellio and L. H. Skibsted, *J. Agric. Food Chem.*, 2000, **48**, 204–212.
37 L. V. Jorgensen, H. J. Andersen and L. H. Skibsted, *Free Radical Res.*, 1997, **27**, 73–87.
38 L. V. Jorgensen and L. H. Skibsted, *Free Radical Res.*, 1998, **28**, 335–351.
39 A. Ben-Aziz, G. Britton and T. W. Goodwin, *Phytochemistry*, 1969, **12**, 2759–2764.
40 H. E. Gottlieb, V. Kotlyar and A. Nudelman, *J. Org. Chem.*, 1997, **62**, 7512–7515.
41 A. Mikkelsen and L. H. Skibsted, *Z. Lebensm.-Unters. Forsch.*, 1995, **200**, 171–177.